Supplementary information
(Appendix Figures)

N-acetyl-L-tyrosine is an intrinsic triggering factor of mitohormesis in stressed animals

Takashi Matsumura, Outa Uryu, Fumikazu Matsuhisa, Keiji Tajiri, Hitoshi Matsumoto, Yoichi Hayakawa

Correspondence to: hayakayo@cc.saga-u.ac.jp

Appendix Figures

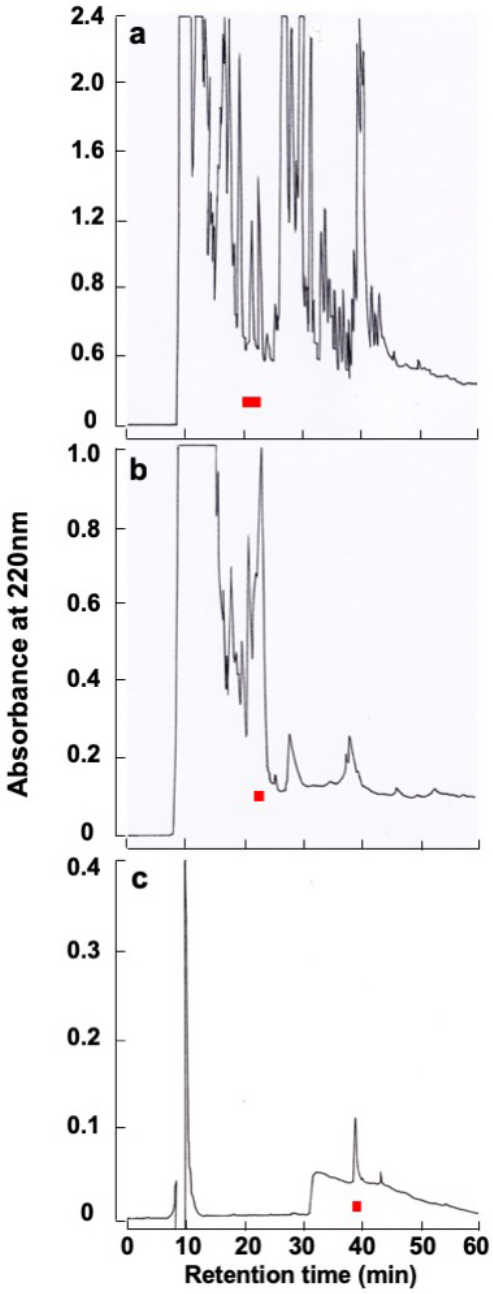

Appendix Figure S1. Purification of the mitohormesis inducer by HPLC. Three analytical HPLC runs using reversed phase columns monitored at 220 nm in combination with heat stress tolerance assays resulted in an active fraction indicated by red underlines.

(a) Mightysil RP-18 GP, 250 x 4.6 mm (5µm) (Kanto Chemical Co., Japan) (b) Mightysil NH_2, 250 x 4.6 mm (5µm) (Kanto Chemical Co., Japan) (c) J-Pak Symphonia C18, 250 x 4.6 mm (5µm) (Jasco Engineering Co., Japan).

a

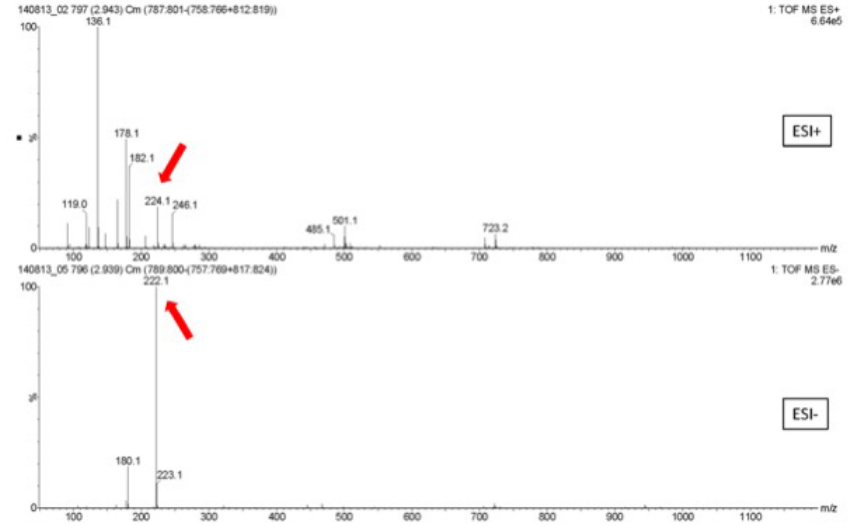

b

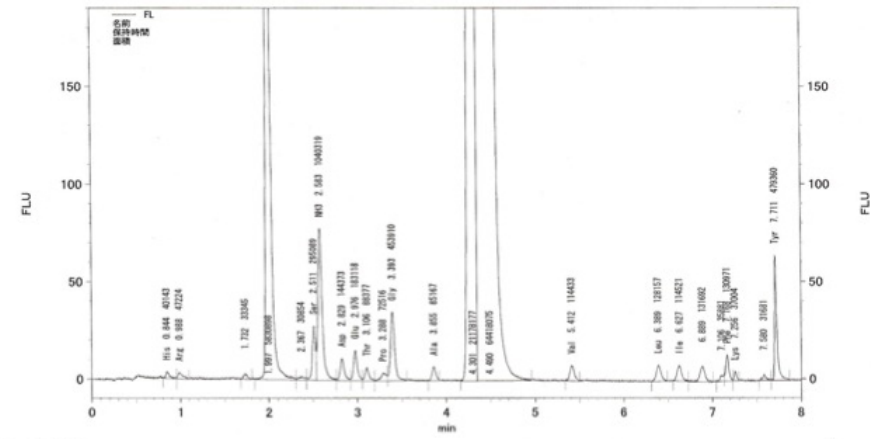

FL結果

名前	保持時間	高さ	面積	ESTD 濃度	単位
His	0. 844	13848	40143	0. 107	pmol
Arg	0. 988	12703	47224	0. 131	pmol
Ser	2. 511	111283	295089	0. 896	pmol
NH3	2. 583	311896	1040319	16. 466	pmol
Asp	2. 829	45308	144373	0. 453	pmol
Glu	2. 976	62398	183118	0. 524	pmol
Thr	3. 106	27709	88377	0. 216	pmol
Pro	3. 288	16161	72516	0. 407	pmol
Gly	3. 393	141299	453910	1. 069	pmol
Ala	3. 855	28432	85167	0. 235	pmol
Val	5. 412	32070	114433	0. 227	pmol
Met				0. 000BDL	pmol
Leu	6. 389	34074	128157	0. 271	pmol
Ile	6. 627	32246	114521	0. 197	pmol
Cys2				0. 000BDL	pmol
Phe	7. 168	54226	130971	0. 198	pmol
Lys	7. 256	19938	37004	0. 127	pmol
Tyr	7. 711	256671	479360	2. 204	pmol
Total		1200262	3454682	23. 728	

Appendix Figure S2. LC-MS analysis and amino acid analysis of mitohormesis inducer molecule. (a) The active peak fraction (Appendix Figure S1c) was analyzed by LC-MS and the protonated molecule was found at m/z 224.1. (b) The same fraction was analyzed by amino acid analyzer (LA8080, Hitachi, Japan) and tyrosine residue was detected as indicated by underline.

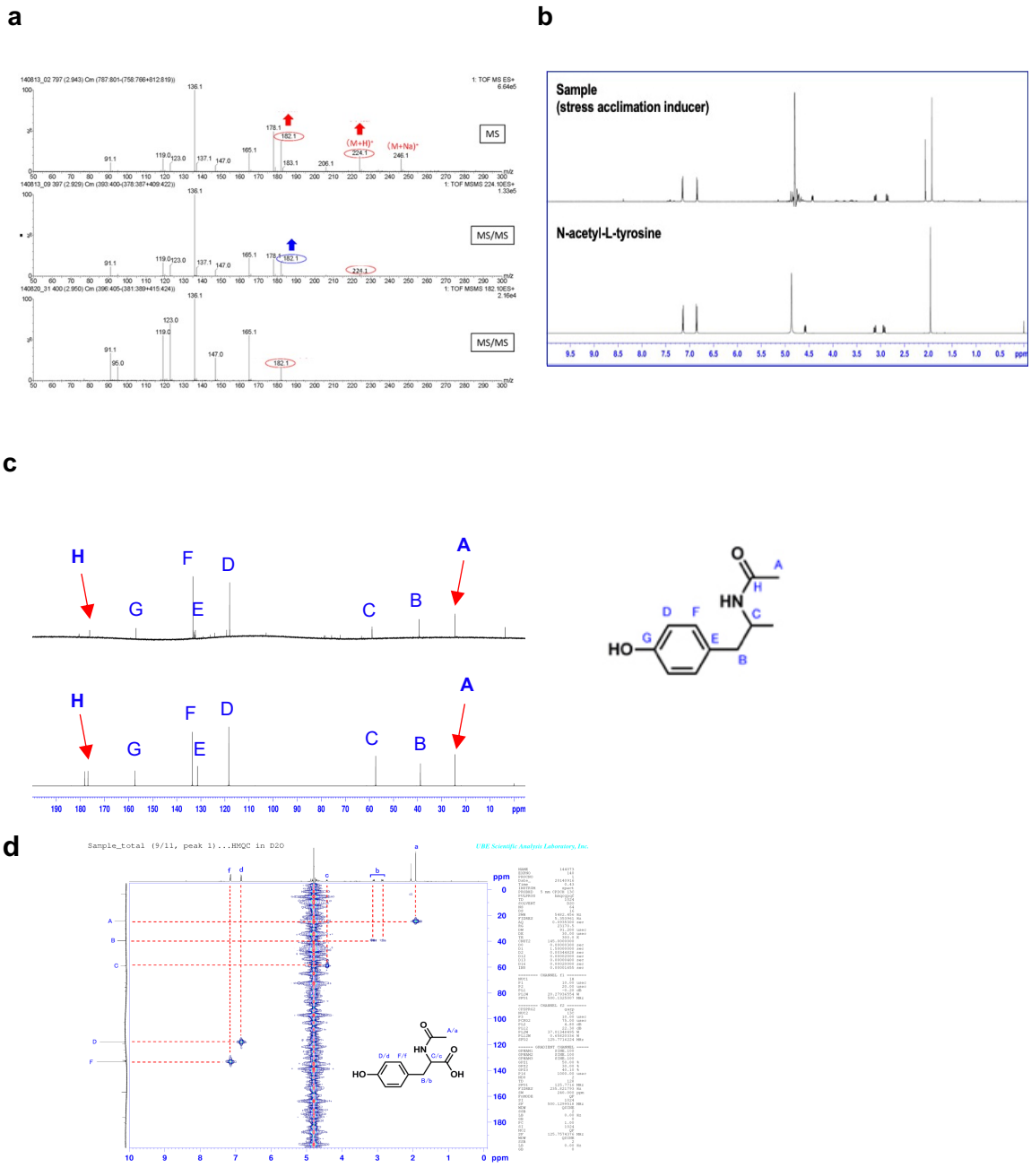

Appendix Figure S3. LC-MS/MS, ^{1}H-NMR, and ^{13}C-NMR analyses of mitohormesis inducer molecule. (a) The precursor ion (Appendix Figure S2) was analyzed by LC-MS/MS, which enabled us to deduce the molecular formula as $C_{11}H_{13}NO_4$. (b) Based on LC-MS/MS analysis, we speculated that the stress acclimation factor could be N-acetyl-L-tyrosine. We compared ^{1}H-NMR spectra between the sample and N-acetyl-L-tyrosine and found that both were almost identical. (c) ^{13}C-NMR analysis identified the carbons (A and H) of the acetyl residue, which are indicated by arrows. (d) HMQC analysis confirmed that the target molecule is N-acetyltyrosine.

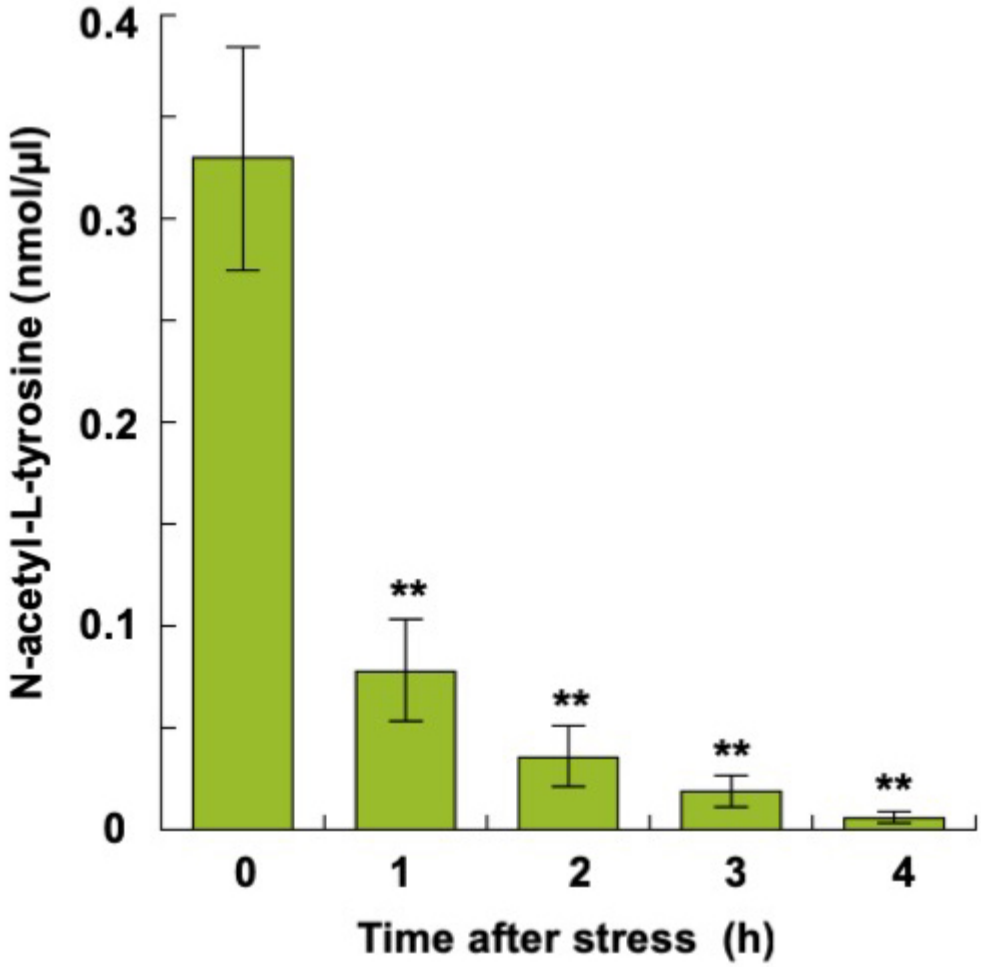

Appendix Figure S4. N-acetyl-L-tyrosine concentration in the plasma of the armyworm larvae after its injection. Each armyworm larva (Day-1 of last instar) was injected with 4 µl of 0.2 µM N-acetyl-L-tyrosine and its hemolymph was then collected at indicated times to measure N-acetyl-L-tyrosine concentrations (data are means ± SEM; n=8). Significant differences are indicated by Tukey's HSD (**P<0.01 vs. zero time).

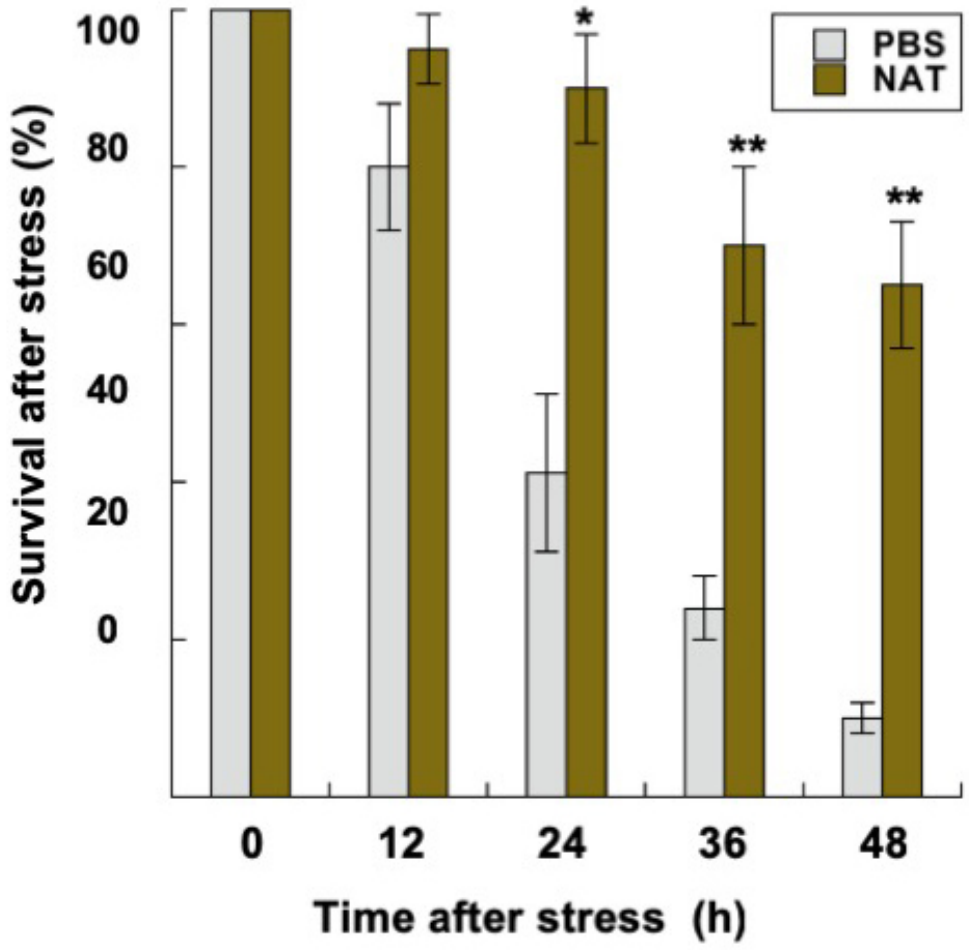

Appendix Figure S5. N-acetyl-L-tyrosine induces heat stress tolerance of silkworm larvae. Each silkworm larva (Day-1 of last instar) was injected with 4 µl of 0.2 µM N-acetyl-L-tyrosine, left at 25°C for 4 h, and exposed to 44°C for 50 min. Survivals were measured at indicated times after heat stress (data are means ± SEM; n=7). Significant differences are indicated by Tukey's HSD (*P<0.05, **P<0.01 vs. zero time).

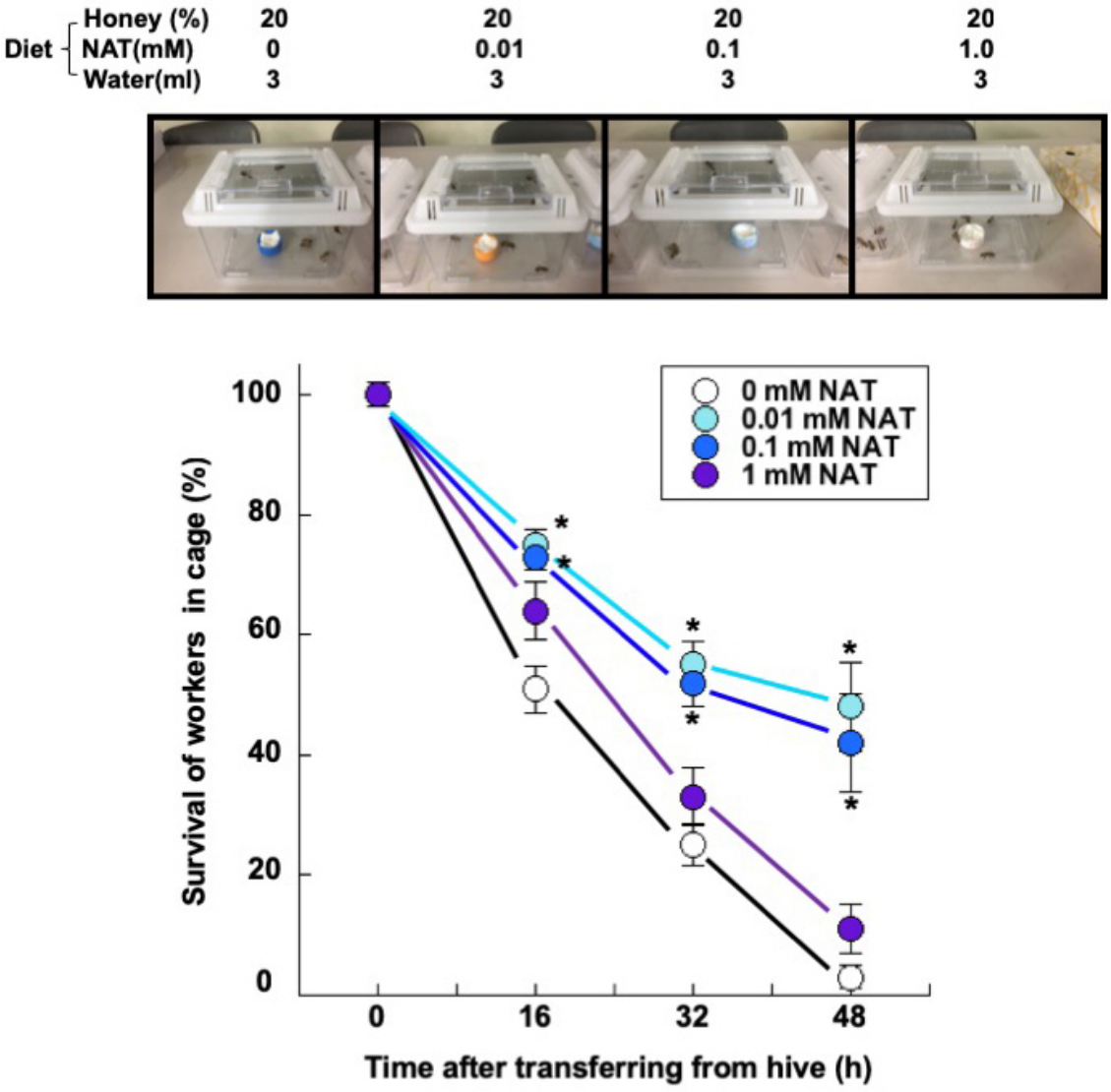

Appendix Figure S6. N-acetyl-L-tyrosine induces stress tolerance of young workers of *Apis mellifela*. Young workers collected from their hive were put into the small cage with honey solution containing different concentrations of N-acetyl-L-tyrosine (NAT) as shown in upper panel. Survivals were measured at indicated times (data are means ± SEM; n=6) (lower panel). Significant differences are indicated by Tukey's HSD (*P<0.05 vs. without NAT). Note that supplementation of honey containing 0.01-0.1 mM NAT significantly increased survivals of test workers.

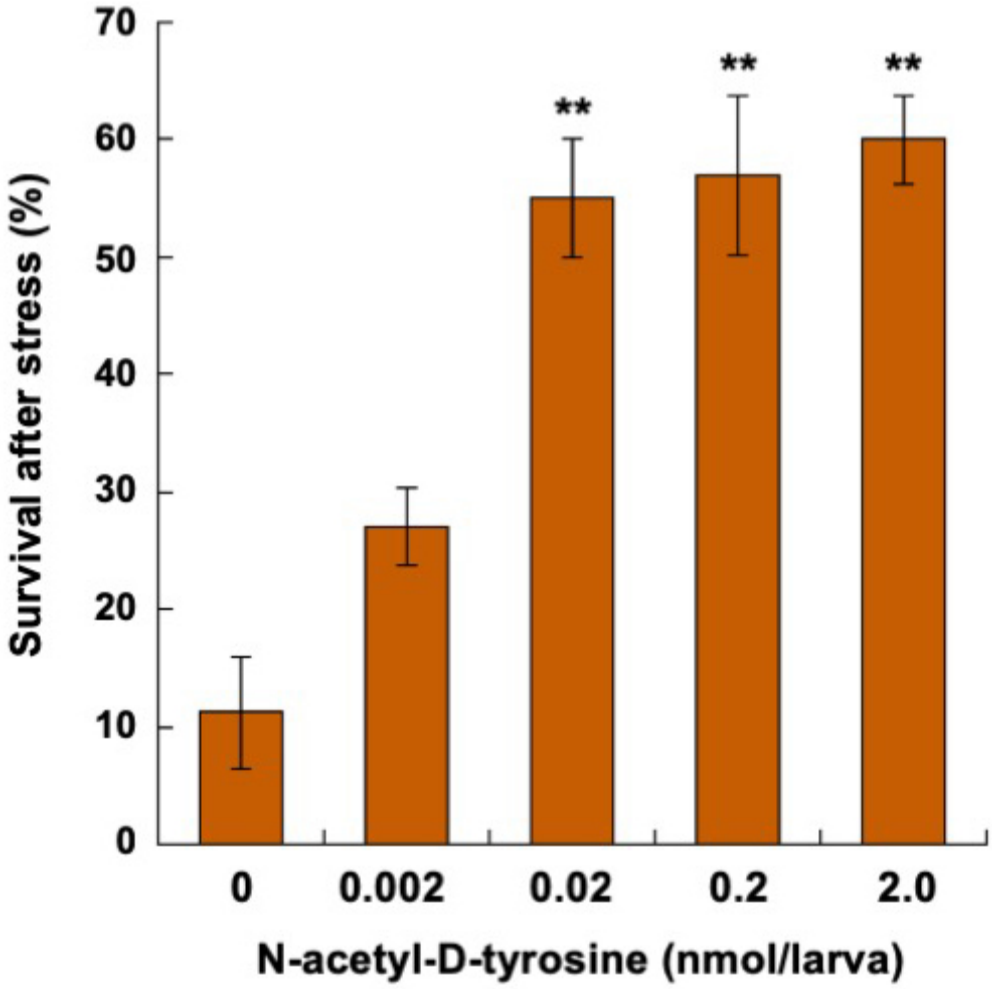

Appendix Figure S7. N-acetyl-D-tyrosine induces heat stress tolerance of the armyworm larvae. Test armyworm larva (Day-1 of last instar) was injected with indicated amounts of N-acetyl-D-tyrosine, left at 25ºC for 4 h, and exposed to 44ºC for 50 min. Survivals were measured 24 h after heat stress (data are means ± SEM; n=8). Significant differences are indicated by Tukey's HSD (**P<0.01 vs. without N-acetyl-D-tyrosine).

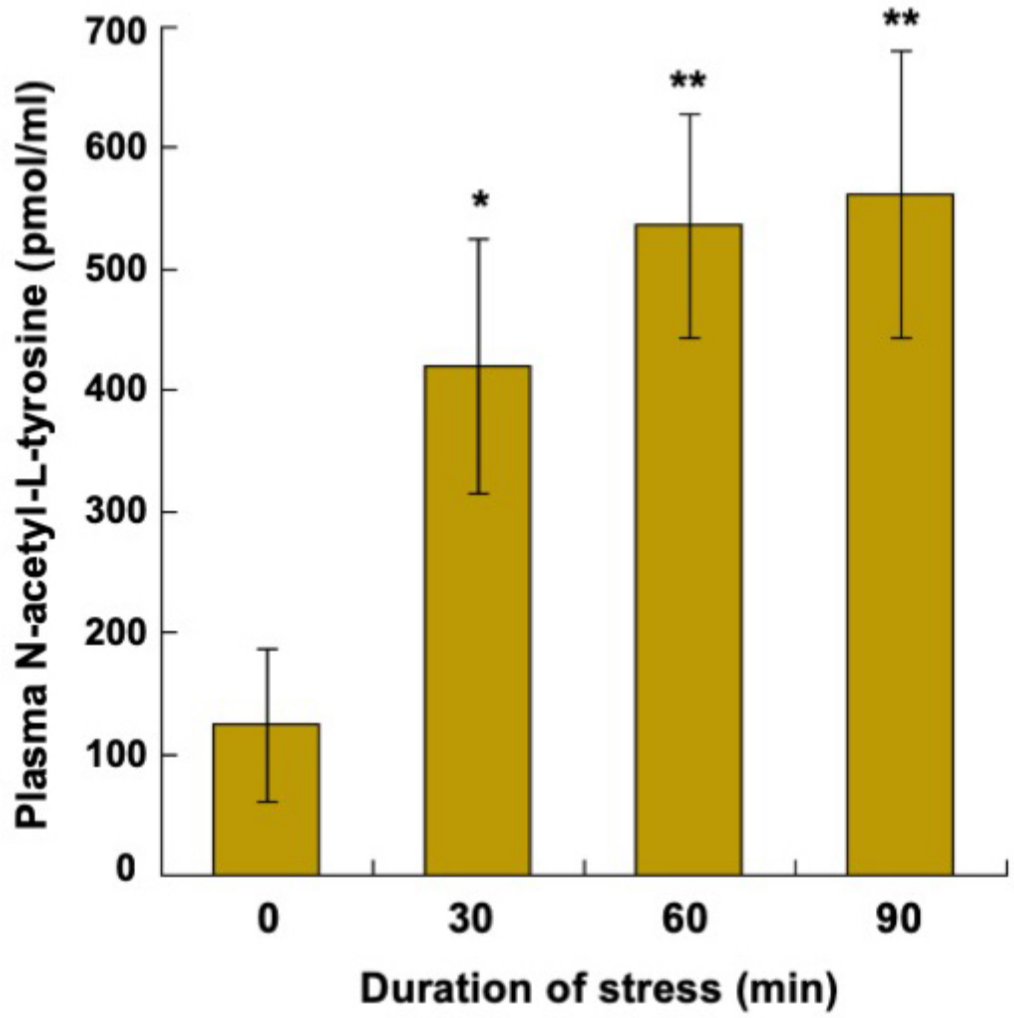

Appendix Figure S8. N-acetyl-L-tyrosine concentrations in the plasma of the armyworm larvae exposed to heat stress. Eighty µl of hemolymph was collected from armyworm larvae (Day-1 of last instar) exposed to 42ºC for indicated periods, immediately mixed with 450 µl 100 mM citrate buffer (pH5.8), and boiled for 3 min. The boiled hemolymph was mixed with 200 µl of 1,2-dichloroethane, and the supernatant after centrifugation at 4ºC for 15 min at 20,000*g* was used to measure N-acetyl-L-tyrosine concentrations by HPLC (data are means ± SEM; n=8). Significant differences are indicated by Tukey's HSD (*P<0.05, **P<0.01 vs. zero time).

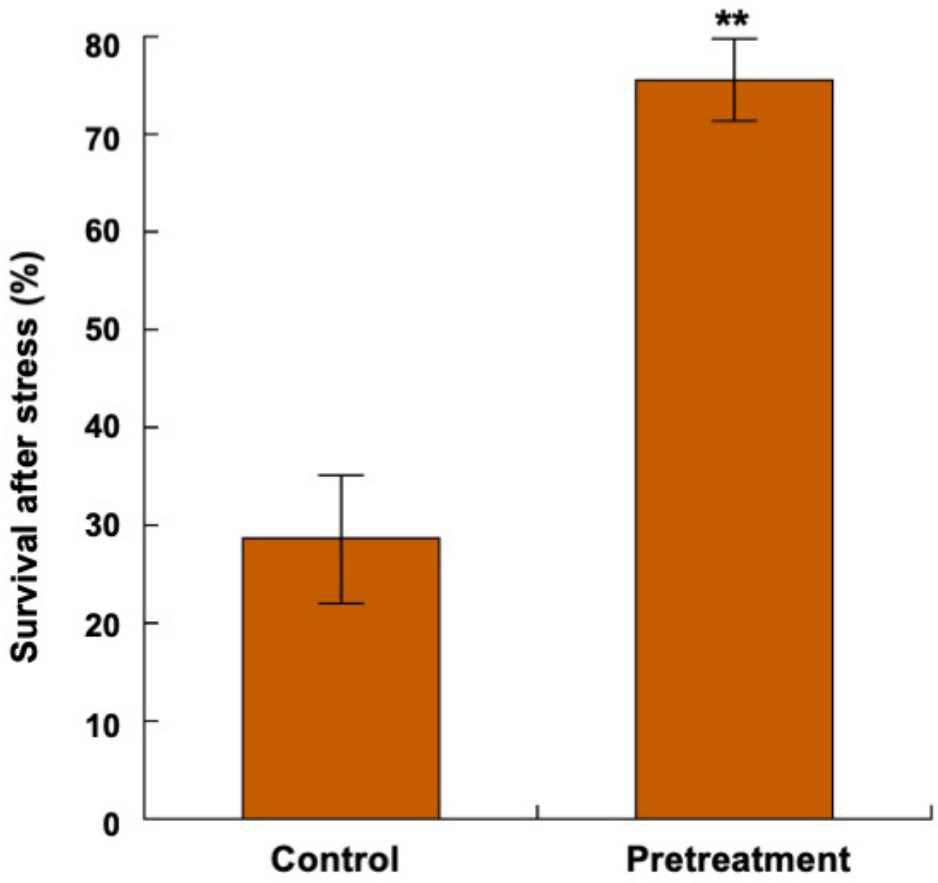

Appendix Figure S9. Pretreatment at mild stress induces heat stress tolerance of *Drosophila* larvae. *Drosophila* larvae (90 h – 100 h after egg-laying) were preheated at 38°C for 30 min, left at 25°C for 30 min, and exposed to 38.5°C for 60 min. Survivals were measured 20 h later (data are means ± SEM; n=6). Significant differences are indicated by Tukey's HSD (**P<0.01 vs. control).

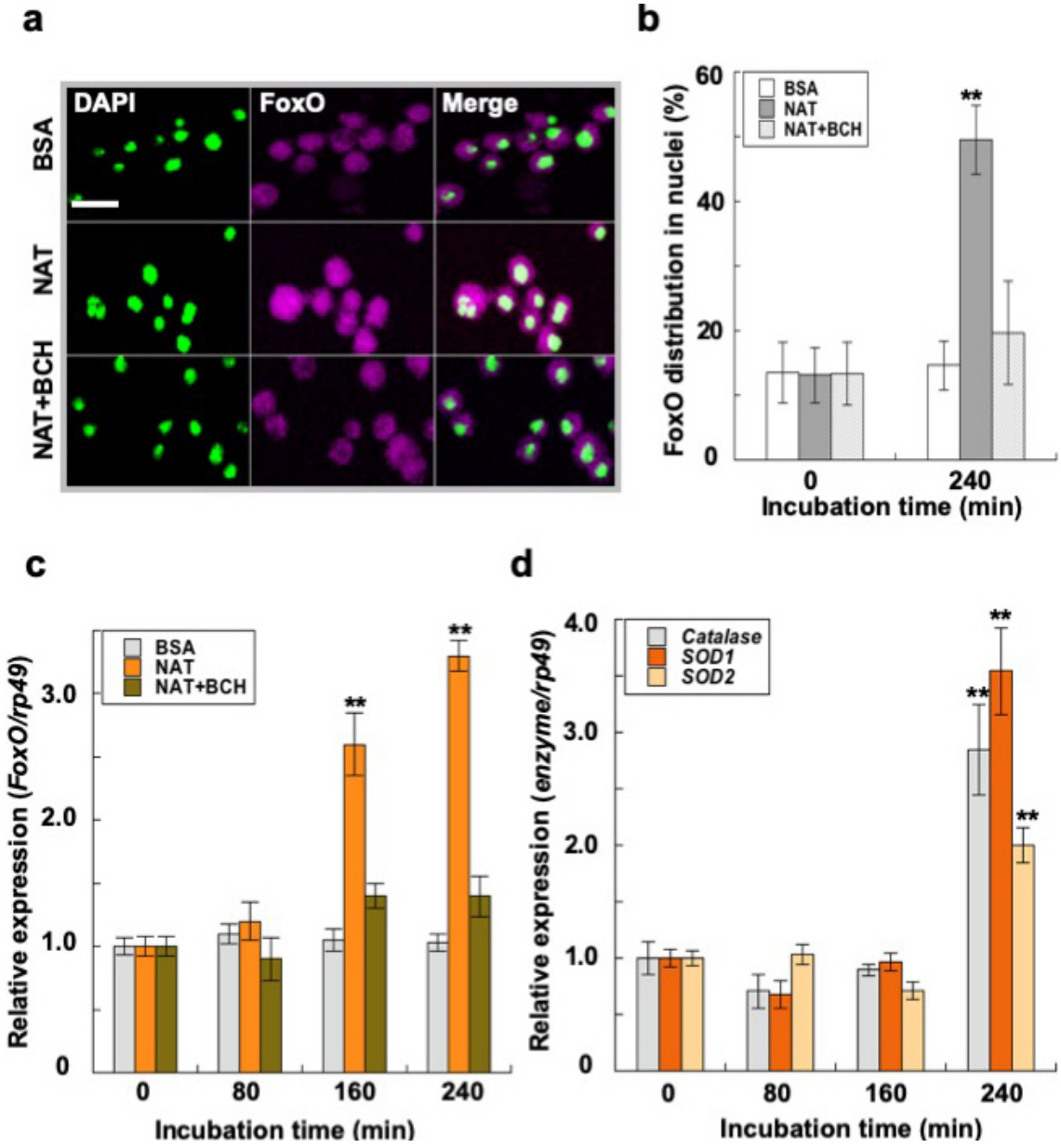

Appendix Figure S10. N-acetyl-L-tyrosine(NAT)-induced signaling pathways in *Drosophila* S2 cells. (a) Representative images of nuclei (left) and FoxO (middle) in *Drosophila* S2 cells incubated with 100 μM BSA, 100 μM NAT, and 100 μM NAT plus 10 mM BCH. White signals in the merged image (right) show the overlap of both signals. Scale bar: 50 μm. (b) Relative whiteness intensities in (a) (data are means ± SEM; n=10). Significant differences are indicated by Tukey's HSD (**P<0.01 vs. BSA). (c) Effects of 100 μM NAT on *FoxO* expression in *Drosophila* S2 cells (data are means ± SEM; n=10). Significant differences are indicated by Tukey's HSD (**P<0.01 vs. zero time). (d) Effects of 100 μM NAT on expression of antioxidant enzymes, *catalase*, *SOD1*, and *SOD2* in S2 cells (data are means ± SEM; n=10). Other explanations are as in (c).

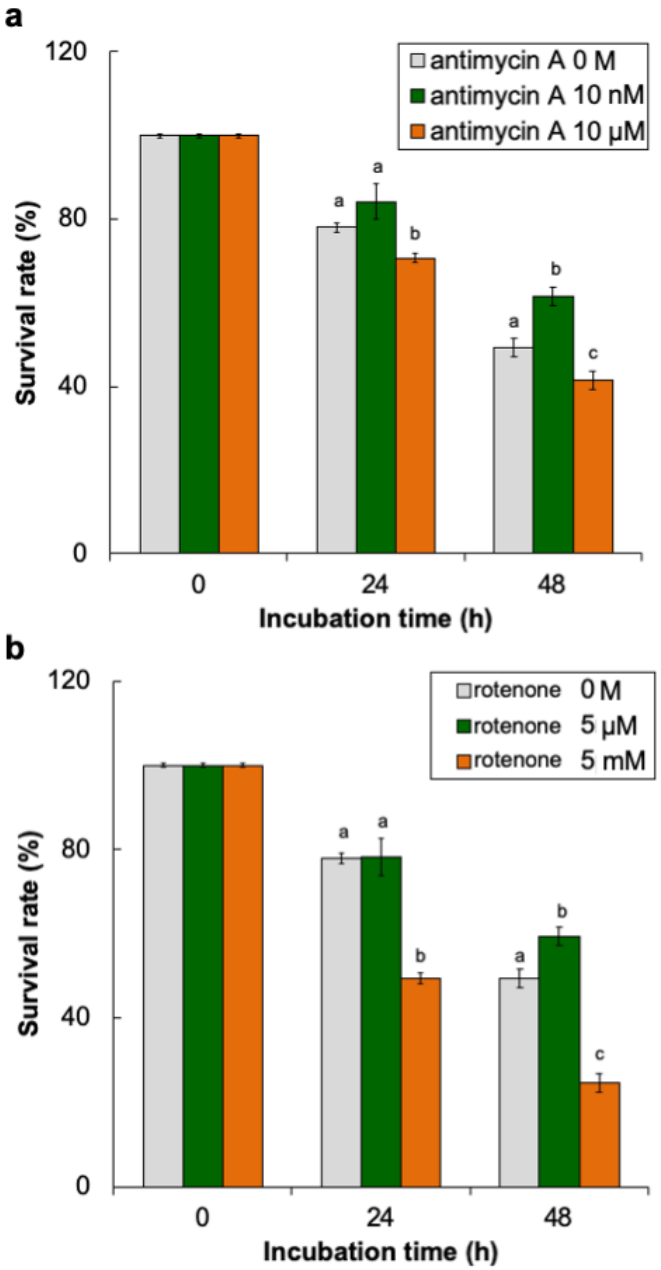

Appendix Figure S11. Survival of *Drosophila* S2 cells pretreated with different concentrations of mitochondrial electron transport chain complex inhibitors. (a) Survival of *Drosophila* S2 cells pretreated with antimycin A after heat stress at 42ºC for 60 min. Different letters above bars represent significant differences indicated by Tukey's HSD [P <0.05 (data are means ± SEM, n=6)]. (b) Survival of *Drosophila* S2 cells pretreated with rotenone after heat stress at 42ºC for 60 min. Other explanations are as in (a).

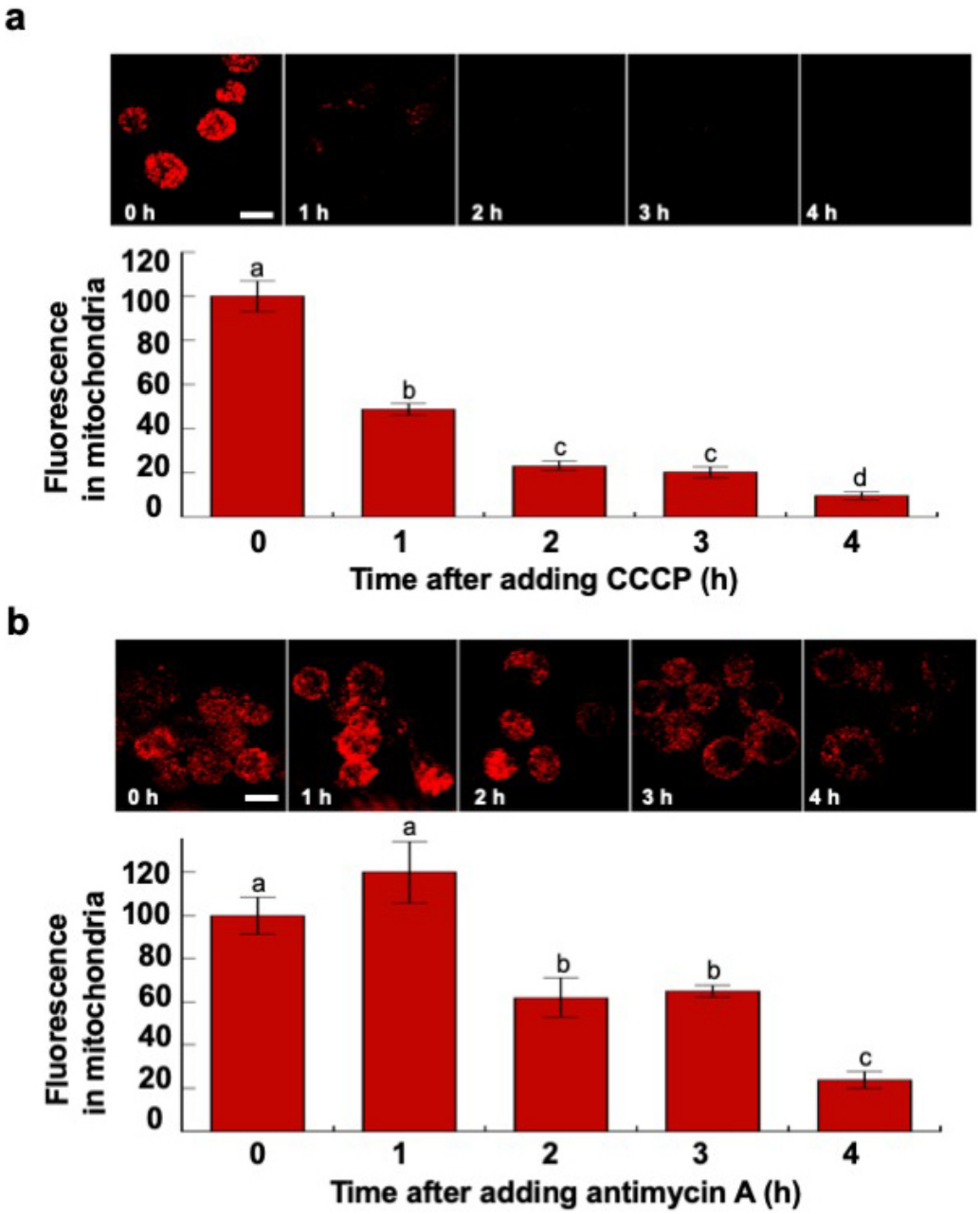

Appendix Figure S12. Effects of chemicals on MitoRed localization in mitochondria of *Drosophila* S2 cells. (a) Representative images of MitoRed localization (upper panel) and relative intensities of MitoRed fluorescence (lower panel) in mitochondria of S2 cells after adding 10 μM CCCP. Scale bar: 20 μm. Relative intensities of MitoRed fluorescence were quantified by microplate reader. Different letters above bars represent significant differences indicated by Tukey's HSD [$P < 0.05$ (data are means ± SEM, n=8)]. (b) Representative images of MitoRed localization (upper panel) and relative intensities of MitoRed fluorescence (lower panel) in mitochondria of S2 cells after adding 18 μM antimycin A. Other explanations are as in (a).

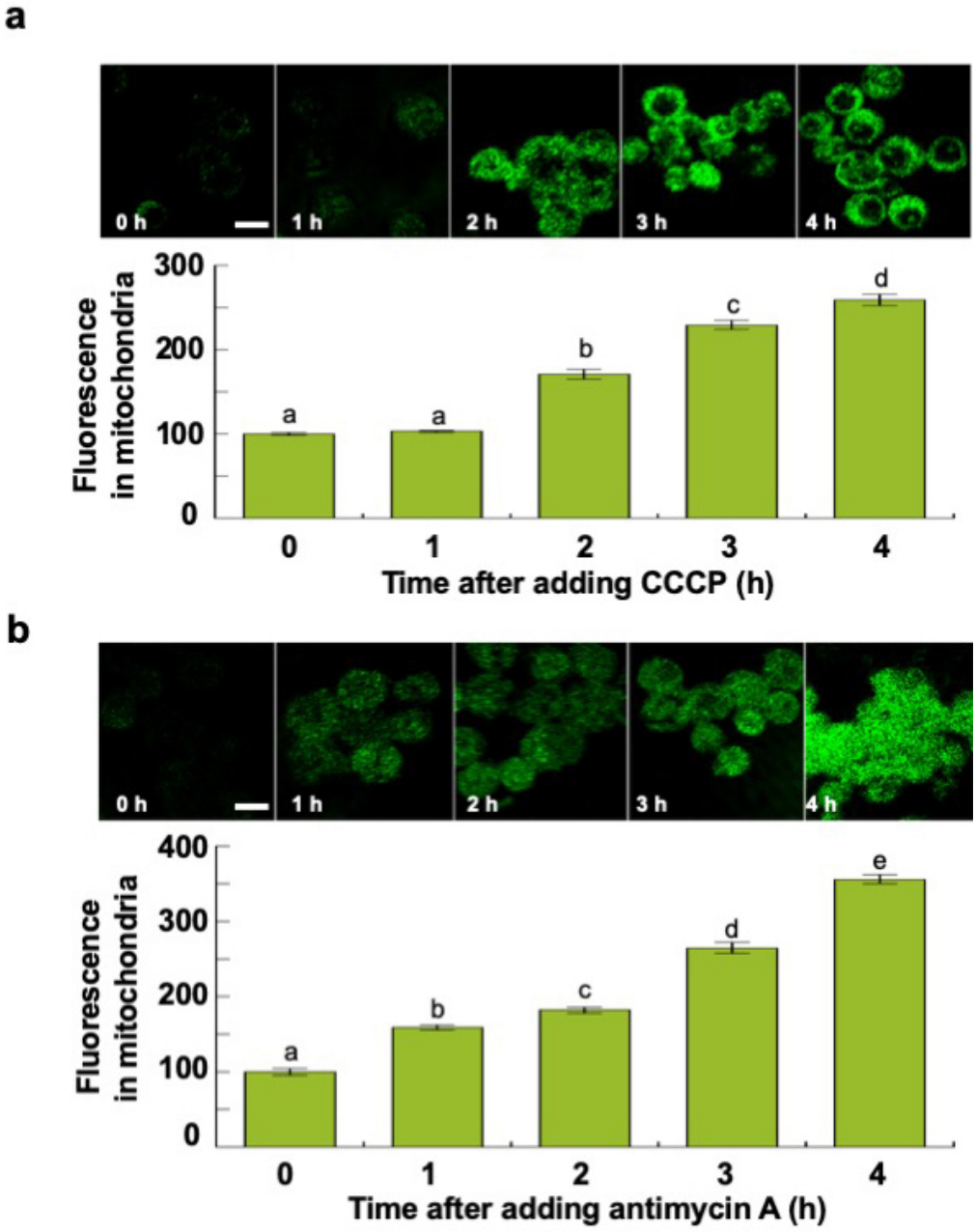

Appendix Figure S13. Effects of chemicals on ROS production in mitochondria of *Drosophila* S2 cells. (a) Representative images of mitochondrial ROS (mROS) (upper panel) and relative intensities of mROS fluorescence (lower panel) of S2 cells pretreated with 10 μM CCCP. mROS fluorescence intensities were quantified by microplate reader. Scale bar: 20 μm. Different letters above bars represent significant differences indicated by Tukey's HSD [$P < 0.05$ (data are means ± SEM, n=8)]. (b) Representative images of mROS (upper panel) and relative intensities of mROS fluorescence (lower panel) of S2 cells pretreated with 18 μM antimycin A. mROS fluorescence intensities were quantified by microplate reader. Other explanations are as in (a).

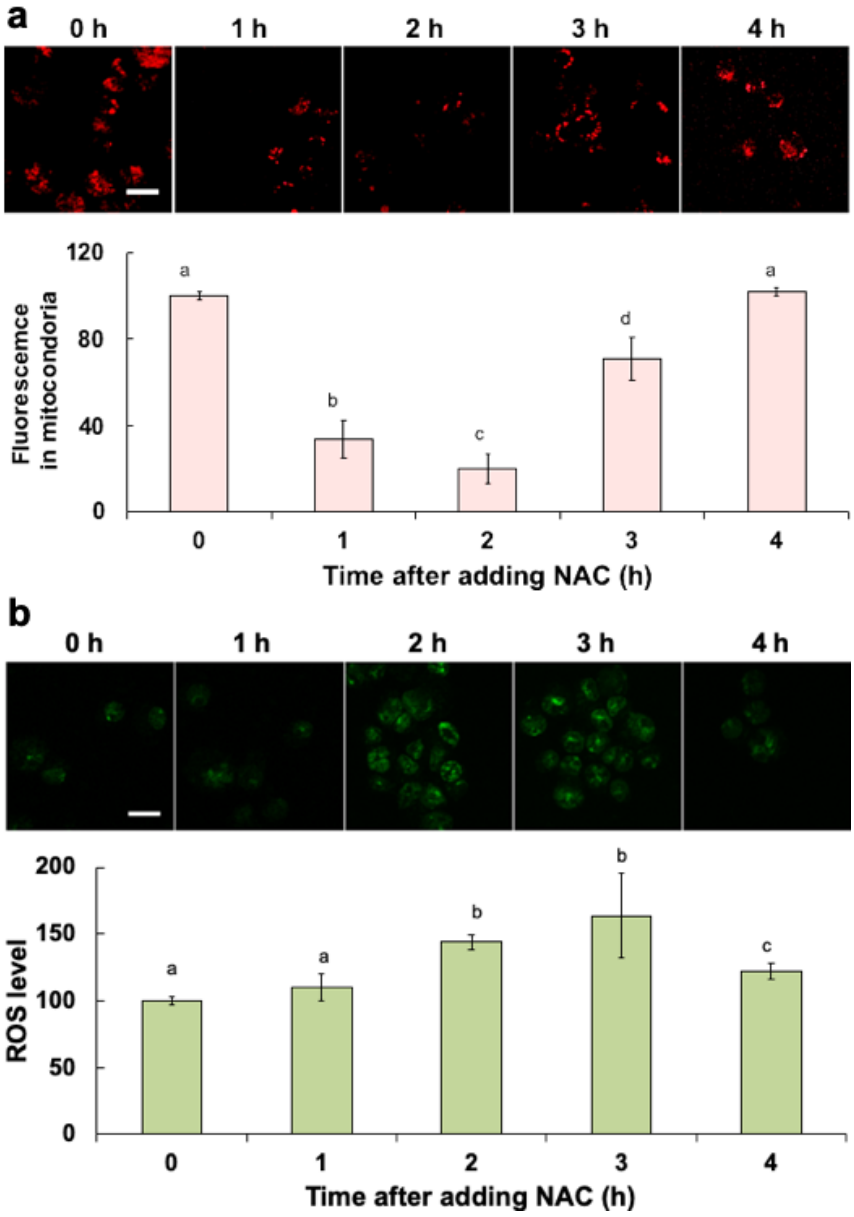

Appendix Figure S14. Effects of N-acetyl-L-cysteine (NAC) on MitoRed localization and ROS production in mitochondria of *Drosophila* S2 cells. (a) Representative images of MitoRed localization (upper panel) and relative intensities of MitoRed fluorescence (lower panel) in mitochondria of S2 cells pretreated with 100 μM NAC. Relative intensities of fluorescence were quantified by microplate reader Different letters above bars represent significant differences indicated by Tukey's HSD [$P < 0.05$ (data are means ± SEM, n=8)]. Scale bar: 20 μm. (b) Representative images of mitochondrial ROS (mROS) (upper panel) and intensities of mROS fluorescence (lower panel) in S2 cells pretreated with 100 μM NAC. Other explanations are as in (a).

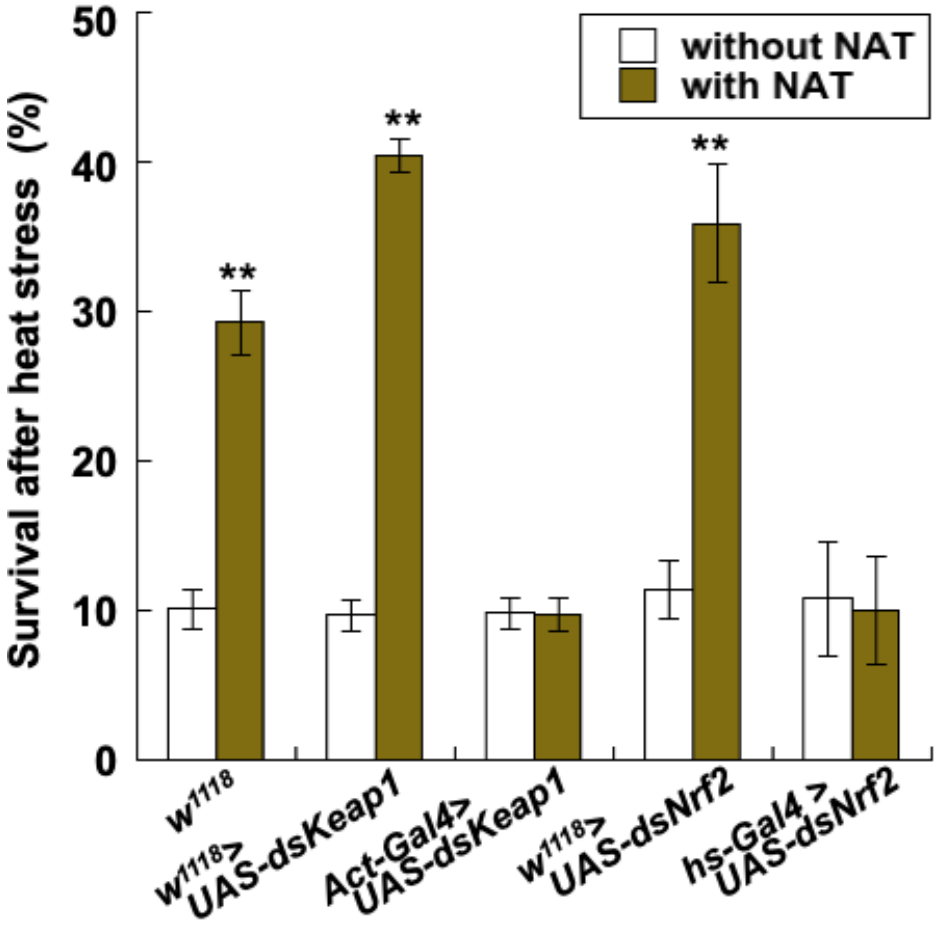

Appendix Figure S15. Effects of *Keap1* and *Nrf2* RNAi on NAT-induced thermotolerance of transgenic *Drosophila* larvae. *Keap1* and *Nrf2* were respectively knocked down using the *Actin-Gal4* and *hs-Gal4* drivers (data are means ± SEM; n=6). Significant differences are indicated by Tukey's HSD (**P<0.01 vs. without NAT). The *hs-Gal4* driver was used for *Nrf2* RNAi because ubiquitous *Nrf2* knockdown with *Actin-Gal4* resulted in embryonic lethality. Test larvae were fed with 2 μmol NAT/g-diet for 24 h before heat stress at 40°C for 30 min. Note that neither *Keap1 RNAi* nor *Nrf2 RNAi* larvae showed NAT-induced thermotolerance.

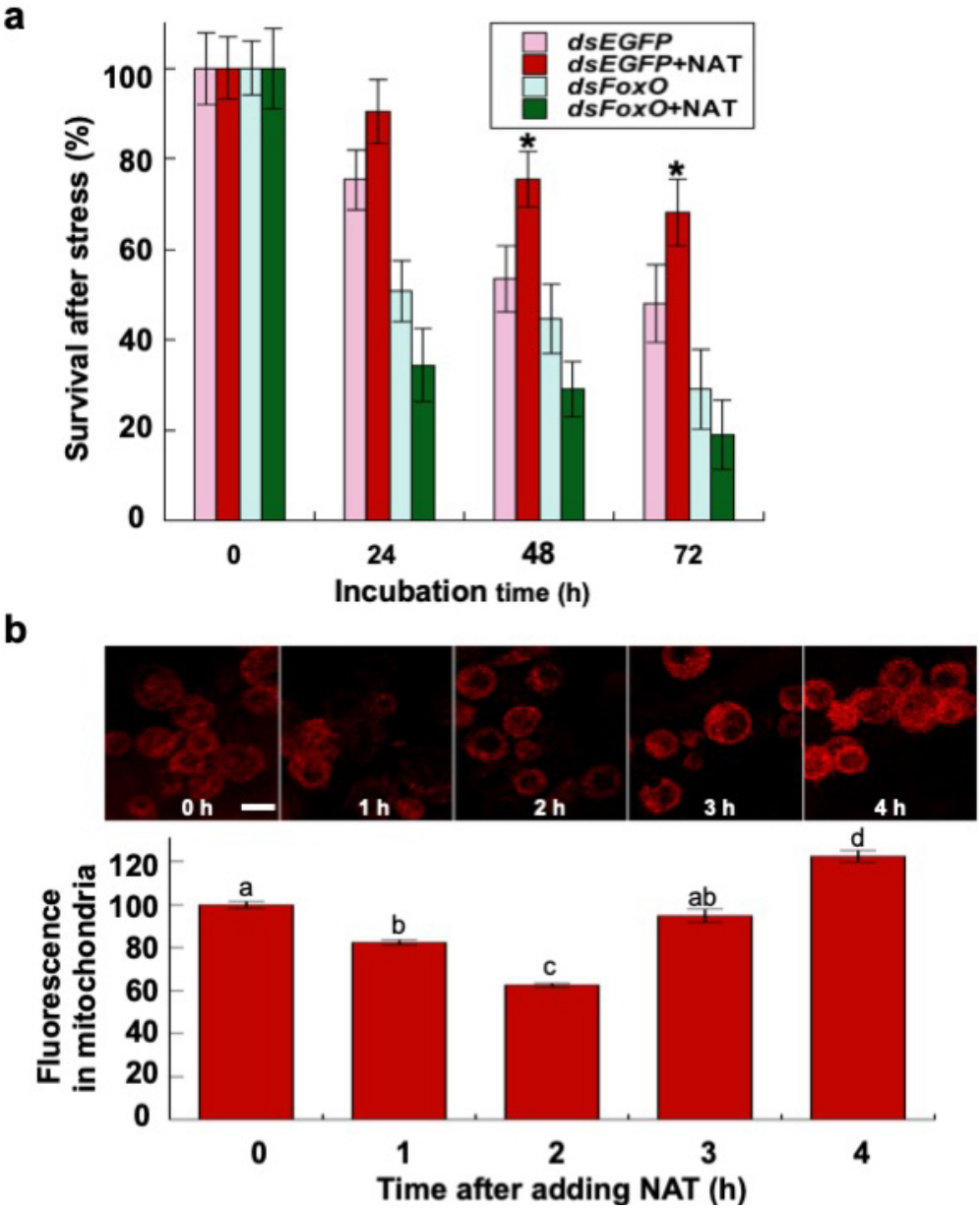

Appendix Figure S16. Effects of dsRNA targeting of *FoxO* on survival and mitochondria of *Drosophila* S2 cells. (a) Effects of dsRNA targeting of *FoxO* on survival of *Drosophila* S2 cells with or without 100 μM N-acetyl-L-tyrosine (NAT) (data are means ± SEM; n=8). Significant differences are indicated by Tukey's HSD (*P<0.05 vs. without NAT). The negative effects of NAT treatment observed in *FoxO* RNAi S2 cells after 24 h might be due to its weak toxicity. (b) Representative images of MitoRed localization in mitochondria of *FoxO* RNAi S2 cells after adding 100 μM NAT. Scale bar: 20 μm (upper panel). Relative intensities of MitoRed fluorescence in mitochondria were quantified by microplate reader (lower panel). Different letters above bars represent significant differences indicated by Tukey's HSD [P <0.05 (data are means ± SEM, n = 8)].

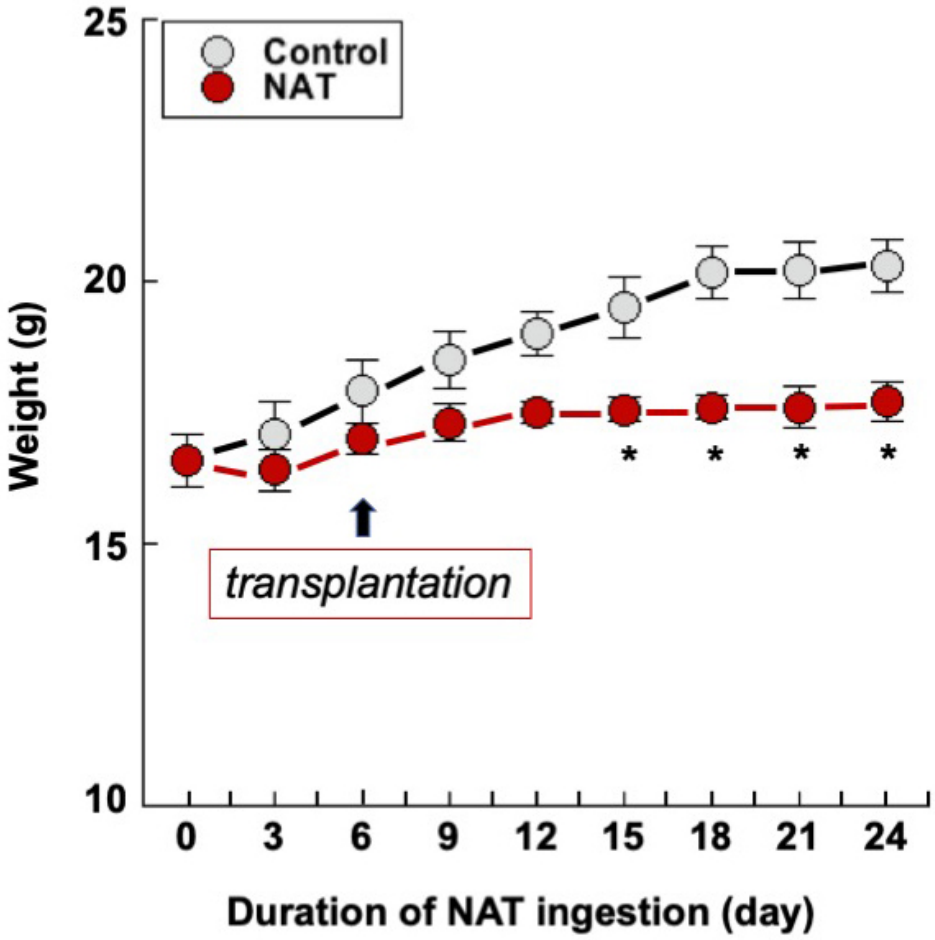

Appendix Figure S17. Administration of N-acetyl-L-tyrosine suppresses body weight gain of nude mice. N-acetyl-L-tyrosine was administered to each test mouse (BALB/cSlc-*nu/nu*) in drinking water at approximately 0.5g/kg of body weight per day and mouse body weights were measured at indicated days (data are means ± SEM; n=5). Significant differences are indicated by Tukey's HSD (*P<0.05 vs. control). Following N-acetyl-L-tyrosine administration for 7 days, HCT116 cells were transplanted into test mice.